

Division - Soil Processes and Properties | Commission - Soil Physics

Estimating lateral flow in double ring infiltrometer measurements

Daniel Boeno⁽¹⁾ , Paulo Ivonir Gubiani^{(1)*} , Quirijn de Jong Van Lier⁽²⁾  and Rodrigo Pivoto Mulazzani⁽¹⁾ 

⁽¹⁾ Universidade Federal de Santa Maria, Departamento de Solos, Santa Maria, Rio Grande do Sul, Brasil.

⁽²⁾ Centro de Energia Nuclear na Agricultura, Universidade de São Paulo, Piracicaba, São Paulo, Brasil.

ABSTRACT: The steady infiltration rate of soil profiles is commonly determined for irrigation and soil conservation planning, but the divergence of methods reduces the reliability of measurements. In this study, the steady infiltration rate measured with a double ring infiltrometer (i_{sr-dri}) in different layers of a soil profile was compared between layers and with the steady vertical saturated flow rate estimated by the Richards equation (i_{sr-hy}). The measurements of i_{sr-dri} at the top of the A, E, and Bt horizons were compared to each other and also compared with the i_{sr-hy} to detect the occurrence of lateral flow in double ring infiltrometer measurements. The i_{sr-dri} in the A horizon (236 mm h^{-1}) was around 10 times higher than in the Bt horizon (20 mm h^{-1}), which implies in a lateral flow of almost 90 % in the surface horizon. The occurrence of lateral flow in double ring infiltrometer measurements was also shown by comparing i_{sr-dri} with the vertical saturated flow rate estimated with the Richards equation, i_{sr-hy} . The main conclusion is that i_{sr-dri} measured at the soil surface overestimates the steady infiltration rate of soil profiles when underlying horizons are less permeable and more restrictive to water flow. In these cases, the use of an effective saturated hydraulic conductivity of the soil profile would imply inaccurate planning of drainage, irrigation, and soil conservation designs.

Keywords: steady infiltration rate, modeling, hydrus-1D.

* **Corresponding author:**

E-mail: paulogubiani@gmail.com

Received: March 04, 2021

Approved: April 29, 2021

How to cite: Boeno D, Gubiani PI, Van Lier QJ, Mulazzani RP. Estimating lateral flow in double ring infiltrometer measurements. Rev Bras Cienc Solo. 2021;45:e0210027.

<https://doi.org/10.36783/18069657rbcsc20210027>

Editors: José Miguel Reichert  and João Tavares Filho .

Copyright: This is an open-access article distributed under the terms of the Creative Commons Attribution License, which permits unrestricted use, distribution, and reproduction in any medium, provided that the original author and source are credited.



INTRODUCTION

Infiltration of water into the soil is limited by a dynamic threshold rate termed infiltration capacity (i_c , mm h⁻¹) (Hillel, 2004). A water supply rate from precipitation or irrigation exceeding i_c cannot fully infiltrate and will partially turn into a runoff. Thus, soil use and irrigation management should consider i_c to prevent runoff and the consequent erosion and environmental degradation (Youngs, 1991; Liu et al., 2019; Miyata et al., 2019).

The time-space variability of i_c is due to its dependence on the intrinsic soil permeability and gradients of energy acting on water, which are time-space variables as well. Methods using devices such as tension infiltrometer, permeameter and/or pressure infiltrometer, rainfall simulator, and double ring infiltrometer can be used to evaluate i_c and its variability. Due to its low cost and ease of use, the double ring infiltrometer is a frequently used method (Pott and De Maria, 2003; Arriaga et al., 2009; Fatehnia et al., 2016; Minosso et al., 2017; Silva et al., 2017; Owuor et al., 2018; Bonetti et al., 2019; Fernández et al., 2019; Liu et al., 2019; Schwartz et al., 2019; Sithole et al., 2019).

When a double ring infiltrometer (DRI) field test is performed on an initially unsaturated soil, i_c tends to decrease exponentially over time and, asymptotically, reaches a quasi-steady rate (i_{sr-dr} , mm h⁻¹) (ASTM, 2009). A similar infiltration rate curve can be simulated with the one-dimensional form of the Richards equation for variably-saturated water flow in an initially unsaturated vertical soil column by maintaining a water layer with a negligible hydraulic pressure on its surface and allowing a free drainage at its bottom. This kind of simulation shows that the water flow rate entering the surface of the soil column decreases exponentially over time and asymptotically reaches a steady rate when the entire soil column becomes saturated (Šimůnek et al., 2012). In this condition, the matric gradients of energy become zero, and the steady flow rate in any cross-section area along the soil column is the same and numerically equal to the hydraulic conductivity of the saturated soil column. Furthermore, if several simulations are performed in a same soil column with different initial water contents, all infiltration rate curves will converge to the steady rate which is numerically equal to the saturated hydraulic conductivity (Hillel, 2004).

If the water from the inner ring infiltrates vertically without lateral deviations in any part of the soil profile during the DRI test, the flow conditions in the soil profile would be equal to those in the simulations. Based on these assumptions, it is considered that i_{sr-dr} is an estimate of the hydraulic conductivity of the saturated soil profile (Bouwer, 1986; Sales et al., 1999; Reynolds et al., 2002; Bodhinayake et al., 2004). Thus, i_{sr-dr} is supposed to be the lower limit of i_c in the soil profile (Mbagwu, 1997) and would represent the most restrictive condition to water infiltration. Consequently, it is considered that runoff and erosion are avoided if irrigation rates do not exceed i_{sr-dr} (Chowdary et al., 2006; Vilarinho et al., 2013). Drainage systems (Stovin et al., 2015) and floodwater containment terraces (Kovář et al., 2016) are also planned considering that i_{sr-dr} corresponds to the hydraulic conductivity of the saturated soil profile. Furthermore, i_{sr-dr} has been also used to indicate the potential runoff and erosion risk associated with different soil use and management (Sidiras and Roth, 1986).

However, the occurrence of lateral flow of water infiltrating from the inner ring is almost never evaluated in DRI tests in the field (Zhang et al., 2016). If i_{sr-dr} is biased by a significant amount of lateral flow, i_{sr-dr} overestimates the saturated soil profile hydraulic conductivity and the minimum value of i_c in a soil profile. Lateral flow of water infiltrating from the inner ring is expected to occur: (i) if the water infiltrating from the outer ring is insufficient to supply the lateral flow demand of the infiltration bulb (Ahuja et al., 1976; Wu et al., 1997); under this condition, some water from the inner ring would also be driven laterally in the soil profile (Wu et al., 1997); or (ii) if less permeable subsurface layers favor the occurrence of lateral flow on their upper surface (Bouwer, 1986). A more permeable layer overlying a less permeable one is common in naturally layered

soils such as Ultisols and Alfisols with a clay illuviation horizon (B) (Franco, 2010). The presence of compacted and less permeable subsurface layers is also widely reported in soils managed under no-till (Drescher et al., 2011; Bonini et al., 2011) or with a plow layer compaction (Håkansson, 1990).

Nevertheless, a hypothesis stating the presence of lateral flow in DRI tests is difficult to be evaluated in the field. In situ quantification of lateral flow from the inner ring is challenging. Although it is possible to install probes and automated systems to measure water content and propagation of the infiltration front, it is not easy to determine the contribution of each ring (inner and outer) to the lateral flow. This difficulty implies in the complexity of precisely quantifying saturated flow exclusively in the vertical direction. A field strategy to investigate lateral flow in DRI tests could be by measuring i_{sr-dr} at different depths in the soil profile and comparing their values. If the water from the inner ring infiltrates vertically without lateral deviations in any part of the soil profile during the DRI test, the value i_{sr-dr} should be the same at the different depths. However, if i_{sr-dr} is greater at the soil surface than the i_{sr-dr} measured at a greater depth, it should contain lateral flow. An additional way to investigate if i_{sr-dr} contains lateral flow could be by evaluating if the i_{sr-dr} measured at different depths are greater than the steady, vertical flow rate of the entire saturated soil profile estimated with the one-dimensional form of Richards equation. Combining these two strategies, relevant information can be retrieved about the occurrence of lateral flow in DRI measurements. In this study, we aimed to test the hypothesis that i_{sr-dr} measured at the surface with DRI can contain a significant amount of lateral flow. We used both mentioned strategies to do so.

MATERIALS AND METHODS

Study site

Experimental determinations were performed at an experimental area of the Federal University of Santa Maria - RS (29° 43' 14" S and 53° 42' 18" W; altitude 110 m a.s.l.). The soil is a Typic Paleudult (Soil Survey Staff, 2014), which corresponds to an *Argissolo Vermelho Distrófico arênico* according to Brazilian Soil Classification System (Santos et al., 2013), under no-till management for approximately 7 years. The site was especially suitable because it features a soil profile with a more permeable layer overlying a less permeable one.

Double ring infiltrometer tests

The DRI tests (0.20 m inner ring diameter and 0.40 m outer ring diameter) were performed on the nine experimental plots between May 31, 2018 to June 22, 2018, at the top of A₁, E₁, and B horizons. All tests were performed when soil water content was around field capacity (two to four days after rainfall). Initially, the two rings were inserted into the soil surface to a depth of 0.10 m, and the infiltration rate was determined maintaining a constant head of 0.05 m, according to the methodology described by Reynolds et al. (2002). The amount of infiltrated water was recorded at intervals of 5 min. The duration of each test was between 1.0 and 1.75 h, and they were concluded when at least five successive readings indicated that the infiltration rate had approached its quasi-stead rate i_{sr-dr} . The average of the five final observed rates was considered an estimate of i_{sr-dr} . To install the DRI in underlying E₁ and B horizons, trenches were manually opened some days after the previous infiltration measurement. As the water drained from the A horizon increased the water content in the underlying horizons (E and B), the soil profile was left to drain this exceeding water for two to three days. After that, the soil was removed until the bottom of the trench reached the top of the next soil horizon. During the excavation, the bottom surface of the trench was not trampled to avoid soil compaction. The DRI tests in the E₁ and B horizons were performed as aforementioned. The relatively long time to perform the

measurements (May 31 to June 22, 2018) was due to the time needed to allow the soil to dry between tests, sometimes delayed by rainfall.

Soil analyses

The soil horizons were identified by morphological observation, considering color change (visual), texture (sensitivity to touch), and perceived resistance when introducing a knife tip. Soil physical properties were determined in three subdivisions of the A horizon (A_1 , A_2 , and A_3), two of the E horizon (E_1 and E_2), and on the top of the B horizon. In each of these horizons, two undisturbed soil samples were collected in September 2018 with metal rings (0.04 m high, 0.057 m diameter). A disturbed sample was collected as well. The undisturbed samples were saturated by capillarity for 48 h and weighed. Subsequently, the saturated hydraulic conductivity (K_s , mm h^{-1}) was determined with the use of a constant head permeameter, setting the hydraulic head to 2.52 cm. After determining K_s , the samples were oven-dried at 105 °C for 48 h. Total porosity (TP, $\text{m}^3 \text{m}^{-3}$) was considered equal to the measured volumetric water content at saturation, and soil bulk density (BD, Mg m^{-3}) was calculated dividing the sample dry mass by the ring volume. For these properties, its average from the two samples of each horizon was considered. Particle size distribution (clay, silt, and sand contents) was determined with 20 g of sieved (2 mm screen) air-dried disturbed samples, using the pipette method according to Suzuki et al. (2015).

Process-based numerical simulation of infiltration

Infiltration was simulated applying the one-dimensional form of the Richards equation with the software Hydrus-1D (Šimůnek et al., 2013). Hydrus-1D numerically solves the Richards equation for variably-saturated water flow in one-dimension (Equation 1), assuming that the atmospheric phase and water flow by thermal gradients are insignificant.

$$\frac{\partial \theta}{\partial t} = \frac{\partial}{\partial x} \left[K \left(\frac{\partial h}{\partial x} + 1 \right) \right] \quad \text{Eq. 1}$$

In this equation, θ is the volumetric water content ($\text{m}^3 \text{m}^{-3}$); h is the soil pressure head (m); t is time (h); x is the vertical spatial coordinate (m); and K is the hydraulic conductivity (m h^{-1}).

The van Genuchten-Mualem soil hydraulic model without hysteresis was selected in Hydrus-1D to describe the θ - h - K relation in equation 1. Thus, parameters of the van Genuchten water retention curve [saturated and residual water contents (θ_s and θ_r , $\text{m}^3 \text{m}^{-3}$), α (m^{-1}), and n], the pore-connectivity parameter (dimensionless) l , and the saturated hydraulic conductivity K_s are the soil hydraulic parameter required in Hydrus-1D. The measured K_s values were used, but the value of the other parameter was defined by pedotransfer function as described below.

A soil domain with six materials and 1.8 m length was defined, according to the six horizons of profile (A_1 , A_2 , A_3 , E_1 , E_2 , and B) and respective depths (0.00-0.20, 0.20-0.43, 0.43-0.64, 0.64-0.86, 0.86-1.12, and 1.12-1.80 m). Considering the measured values of sand, silt, clay, and BD of the six horizons, the parameters θ_s , θ_r , α , and n of each layer were estimated for the nine plots using the software Rosetta Lite v. 1.1 (Schaap et al., 2001) available in Hydrus 1D. The default value 0.5 suggested in Hydrus-1D for the pore-connectivity parameter l was used for all horizons.

Simulations were performed setting the initial water condition at field capacity, which was defined automatically in Hydrus 1D as a function of van Genuchten water retention parameters and K_s , using the equation of Twarakavi et al. (2009). A permanent positive pressure head of 5 cm was defined as the upper boundary condition and free drainage as the bottom boundary condition. A duration of 30 h was used in all simulations to ensure that the entire domain was saturated and the steady infiltration rate, $i_{\text{sr-hyr}}$, was achieved.

Under steady vertical flow in a saturated, layered soil column, the solution of Richards equation become the serial Darcy flow equation for N layers according to $i_r = (h+Z)/(L_1/K_{s1} + L_2/K_{s2} + \dots + L_N/K_{sN})$. Note that the infiltration rate (i_r) is a function of thickness (L) and saturated hydraulic conductivity (K_s) of each layer, the hydraulic head (h) at the soil surface, and the length of the soil column (Z). The Hydrus steady infiltration rate (i_{sr-hy}) in our study is the steady vertical flow after the soil column became saturated. Thus, $i_{sr-hy} = i_r$, and then the parameters θ_s , θ_r , α , and n were needed just for running Hydrus, but they were irrelevant for determining the i_{sr-hy} . The initial condition (field capacity based on Twarakavi proposition) is irrelevant as well. The water retention curve parameters affect the shape of infiltration rate curves until the onset of steady infiltration rate and the time infiltration rate become steady. For not estimating inconsistent shaped infiltration rate curves, we estimated the θ_s , θ_r , α , and n parameters according to the texture and bulk density of each horizon, using the software Rosetta. However, Hydrus was used to solve a specific problem in our study: to estimate the steady vertical flow in a saturated, layered soil column. Thus, i_{sr-hy} was our target. In this case, K_s was the mandatory parameter, and K_s was measured in all soil profiles and horizons.

Values of i_{sr-hy} and i_{sr-dr} were compared, and their difference was considered an estimate of the lateral flow contained in i_{sr-dr} . The effect of soil horizons on i_{sr-dr} was tested by analysis of variance. Tukey test was used to identify significant differences in the means of i_{sr-dr} , considering $p < 0.05$.

RESULTS

Profile characterization

The E horizons had a lower clay content (about 0.10 kg kg^{-1}) than the A horizon (about 0.20 kg kg^{-1}) (Table 1). A large increase in clay content (increasing to 0.63 kg kg^{-1}) and a decrease in sand and silt contents is observed in the B horizon. These differences in texture implied in step transitions in the profile permeability when the saturation front entered the E and B horizon, as shown in the next sections. The low K_s of the E horizons indicates a restriction on water entering from the A horizons (Table 1). The E horizons are sandy, which could suggest a higher permeability, but their total porosity (TP) was lower, and bulk density (BD) was higher than that of the B horizon and E_2 . Also, their K_s was lower than in the A_1 horizon, where K_s was much higher than in any of the other horizons. According to the standard deviation, variability in TP and BD was low in each horizon, and they did not correlate clearly with K_s .

Quasi-steady infiltration rate of infiltration curves measured with DRI

The quasi-linear slope of the end of measured cumulative infiltration curves corresponds to the quasi-steady infiltration rate i_{sr-dr} , which normally occurred after one to two hours, but earlier in some of them (Figure 1). Empirical infiltration models were not fitted because

Table 1. Physical properties of the Typic Paleudult soil horizons used in this study. Hydraulic conductivity (K_s), bulk density (BD), and total porosity (TP) are shown as mean \pm standard deviation ($N = 18$)

Horizon	Layer m	Clay	Silt	Sand	K_s mm h ⁻¹	BD Mg m ⁻³	TP m ³ m ⁻³
A ₁	0.00–0.20	0.18	0.16	0.66	136 \pm 175	1.59 \pm 0.06	0.37 \pm 0.04
A ₂	0.20–0.43	0.21	0.18	0.61	9 \pm 5	1.65 \pm 0.09	0.35 \pm 0.03
A ₃	0.43–0.64	0.19	0.19	0.62	36 \pm 21	1.60 \pm 0.07	0.39 \pm 0.05
E ₁	0.64–0.86	0.12	0.24	0.64	10 \pm 9	1.73 \pm 0.02	0.36 \pm 0.02
E ₂	0.86–1.12	0.10	0.26	0.64	4 \pm 2	1.84 \pm 0.06	0.34 \pm 0.04
B	1.12+	0.63	0.10	0.27	4 \pm 3	1.55 \pm 0.06	0.42 \pm 0.02

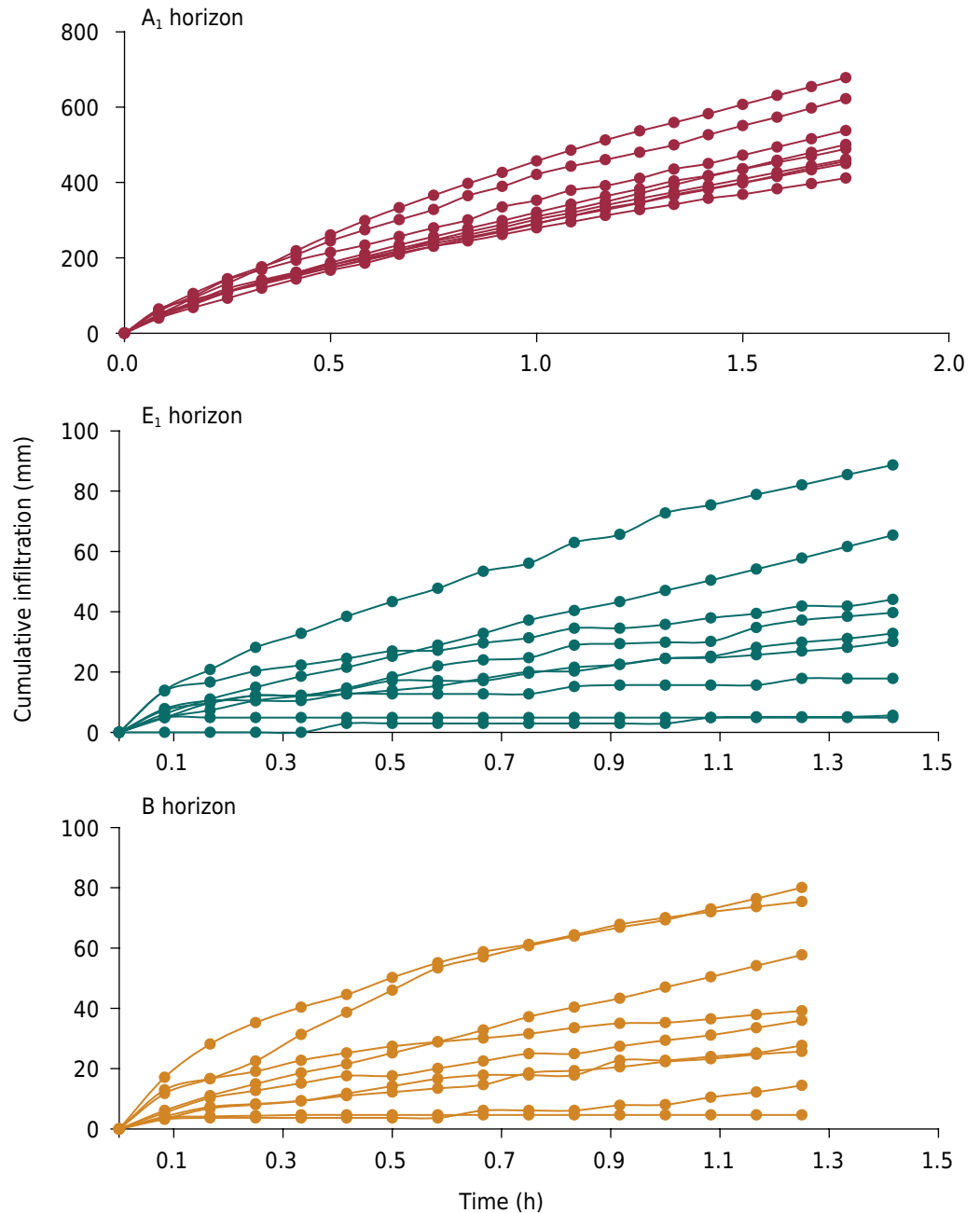


Figure 1. Cumulative infiltration rate versus time measured with a double ring infiltrometer at the top of A_1 , E_1 , and B horizons of nine plots of a Typic Paleudult.

i_{sr-dr} was calculated as average infiltration rate of the five final measurements. Despite the high variability between replication, a notable decrease in the slope of cumulative infiltration curves occurred in curves of E_1 and B horizons.

The average value of infiltration rate of the five final measurements of each infiltration curve, considered an estimate of i_{sr-dr} of each plot, is shown in figure 2. The average values i_{sr-dr} of horizons were statistically different according to the Tukey test ($p = 0.05$). At the top of the A_1 horizon, i_{sr-dr} was an order of magnitude higher than at the top of the E_1 and B horizons (Figure 2).

Quasi-steady infiltration rate of infiltration curves simulated with Hydrus-1D

The nine infiltration rate curves simulated with Hydrus-1D decreased exponentially toward a steady rate, i_{sr-hy} , observed between 7 and 23 h in all simulations (Figure

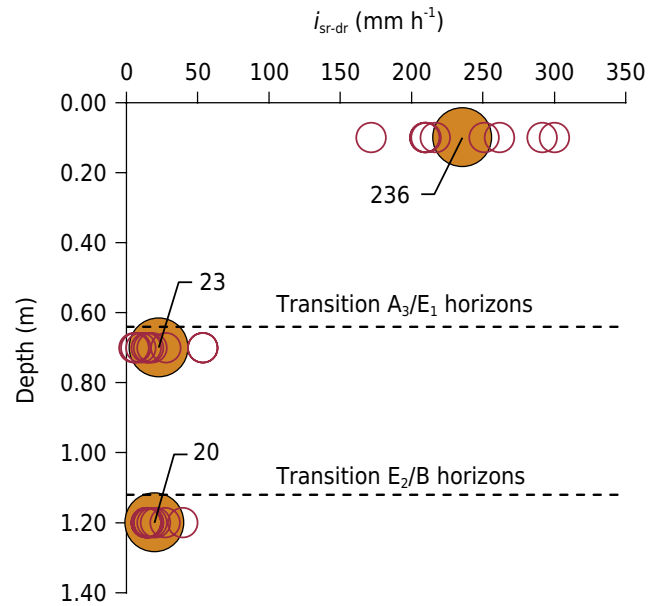


Figure 2. Steady infiltration rate measured with a double ring infiltrometer (i_{sr-dr}) at the top of A_1 , E_1 , and B horizons in nine plots of a Typic Paleudult. Small circles represent individual measurements, larger circles the average value per horizon.

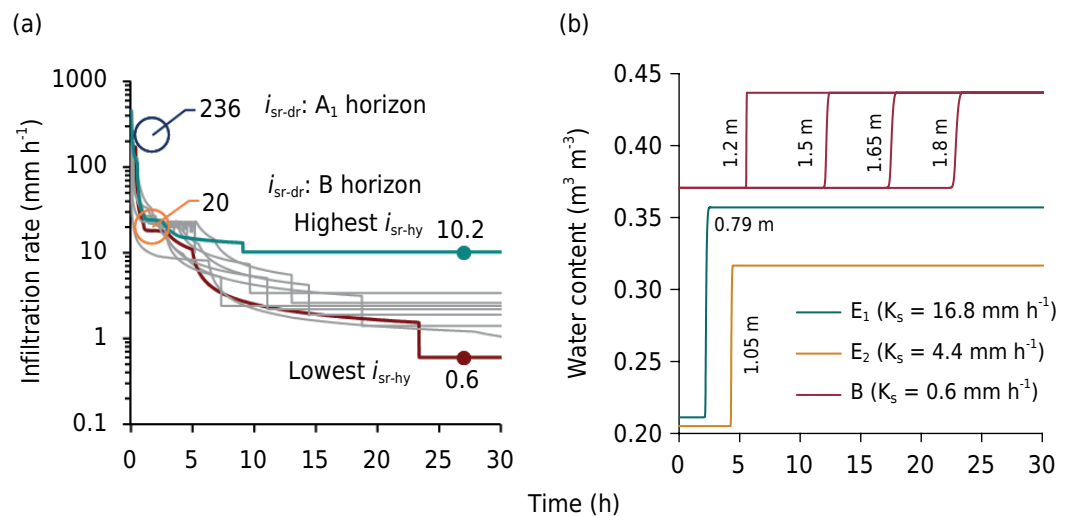


Figure 3. Infiltration rate simulated by Hydrus-1D for all plots and the average of i_{sr-dr} measured with double-ring infiltrometer at top of A_1 and B horizons (a); the upper and lower colored lines correspond to the soil profile less and more restrictive to water infiltration. Water content simulated by Hydrus-1D at different depths along time (b).

3a). The highest i_{sr-hy} (10 mm h^{-1}) was 50 % of i_{sr-dr} of the B horizon (20 mm h^{-1}), and about 4 % of i_{sr-dr} of the A_1 horizon (236 mm h^{-1}). An abrupt decrease of the infiltration rate in some curves indicates a restriction to water flow after the saturation front entered the horizons with lower permeability (E and B) (Table 1). To evaluate the advance of the wetting front, the abrupt change from initial to saturated water content in E and B horizons was shown for the soil profile with the lowest water flow when completely saturated (line converging to i_{sr-hy} of 0.6 mm h^{-1} in figure 3a. For this soil profile, a decrease of the infiltration rate occurred three hours after the onset of the test (Figure 3a), when the wetting front entered the E_1 horizon (Figure 3b). Another step decrease occurred near 5 h from the onset (Figure 3a), when the wetting front entered the B horizon (Figure 3b). A final step occurred at about 23 h (Figure 3a),

when the entire profile reached saturation (Figure 3b), eliminating the pressure head of -1.13 m (corresponding to the initial water content) acting on the wetting front within the B horizon.

DISCUSSION

The average value of i_{sr-dr} in the A₁ horizon was higher than in the deeper horizons (Figure 2). This result and the differences of K_s values in the soil profile (Table 1) show that the soil profiles have a more permeable section overlying a less permeable one, which is a layered condition favorable to test our hypothesis. It seems not to be plausible to attribute the high difference of i_{sr-dr} in the A₁ horizon when compared to the E₁ and B horizons ($\Delta i_{sr-dr} = 216 \text{ mm h}^{-1}$) to factors other than the occurrence of lateral flow in the soil profile (Figure 2). In other words, it is reasonable to assume that i_{sr-dr} measured on top of A₁ horizon largely overestimated the vertical flow in the soil profile. These results are part of the evidences supporting our hypothesis that i_{sr-dr} measured on the soil surface with DRI may contain a significant amount of lateral flow.

Further support to our hypothesis was provided by the Hydrus-1D simulations (Figure 3). A boundary condition for Hydrus-1D simulations is that its steady infiltration rate, i_{sr-hy} , in a saturated soil profile is the saturated vertical flow given by Darcy equation $i_{sr-hy} = q = -K_s (dH/dx)$, which is the solution of equation 1 for a saturated media (Šimůnek et al., 2005). In a saturated media, the parameter governing water flow is K_s . The lowest values of K_s occurred in the E₂ and B horizons (Table 1), which caused some step-decrease in infiltration rate curves (Figure 3a) when the saturation front entered these horizons (Figure 3b). Thus, the range of i_{sr-hy} from 0.6 to 10.2 mm h⁻¹ (Figure 3a) is in agreement with the K_s range of $4 \pm 3 \text{ mm h}^{-1}$ in the B horizon (Table 1), and simulated i_{sr-hy} seems consistent. All estimated i_{sr-hy} were lower than the measured i_{sr-dr} , which shows that lateral flow in DRI tests must have occurred in all horizons. In the A₁ horizon, the magnitude of lateral flow was at least 226 mm h⁻¹.

Although the duration of DRI measurements (between 1.0 and 1.75 h) was different and much shorter than the duration of Hydrus-1D simulation (30 h), the target information in DRI tests is the quasi-steady infiltration rate (Reynolds et al., 2002). Frequently, this target is achieved in DRI tests with a duration shorter than 3.5 h (Uloma et al., 2014; Cunha et al., 2015; Silva et al., 2017; Aboukarima et al., 2018; Zhang et al., 2019). Furthermore, the verification of saturation of the soil profile when infiltration rate approaches quasi-steady rate flow is not mandatory. Taking these considerations into account, the target i_{sr-dr} as a flow rate that tends to a quasi-steady flow rate was satisfactorily met in our experiment (see the quasi-linear slope at the end of the measured cumulative infiltration curves shown in figure 1). Then, even considering long duration infiltration measurements in field conditions in which an additional small reduction in i_{sr-dr} might be observed, the estimated lateral flow would not significantly change.

Our results indicated that i_{sr-dr} is an estimate of vertical flow that could be highly biased by the lateral flow. It is plausible to suppose that the increase in i_{sr-dr} observed in several studies may be caused by an increased lateral flow rather than by an increase in vertical flow. For example, the frequently detected increase in i_{sr-dr} when soil hydraulic properties are changed only in the topsoil, like when changing from conventional to no-till management (Santos et al., 2016; Alhameid et al., 2020), revolving the soil surface by fertilizer shanks (Drescher et al., 2016) and chisels (Camara and Klein, 2005; Prando et al., 2010; Drescher et al., 2016), improvement of bioporosity by the root system (Pagliai, 1993; Azooz and Arshad, 1996; Cessa et al., 2014; Fernández et al., 2019), and reducing animal trampling in integrated crop-livestock systems (Bonetti et al., 2019), is likely a DRI measurement artifact, effect of an increase in lateral flow in the ameliorated topsoil horizon. Although a large i_{sr-dr} at the soil surface favors infiltration in the ameliorated topsoil horizon until

it becomes saturated, the vertical flow after saturation of the more permeable surface layer should be lower than i_{sr-dr} .

The measured value of i_{sr-dr} at the surface is frequently considered to be the effective saturated hydraulic conductivity of the soil profile, K_{ef} (Bouwer, 1986; Reynolds et al., 2002; Bodhinayake et al., 2004). Our results show that this assumption is prone to be highly inaccurate. As a practical consequence, the purpose with projects based on K_{ef} like drainage systems (Stovin et al., 2015) or floodwater containment terraces (Kovář et al., 2016) could not be attained if the i_{sr-dr} used for designing these systems were an inaccurate estimate of K_{ef} .

Our results suggest that i_{sr-dr} may not be considered the lower limit of soil infiltration capacity in the vertical direction nor the upper limit of precipitation rate that will not cause runoff. Hydrus-1D simulations suggested these limits may be much lower than i_{sr-dr} . Using a hydrologic model based on the Richards equation to estimate the lower limit of soil infiltration capacity is a more reliable strategy than using double ring infiltrometer measurements. The latter could be used to compare the effects of soil use and management on the permeability of the surface horizons, but i_{sr-dr} is not a reliable measurement to assess saturated vertical flow in the entire soil profile.

CONCLUSIONS

A significant amount of lateral flow occurs during infiltration rate measurements with a double ring infiltrometer (i_{sr-dr}) at the soil surface with underlying horizons with lower permeability. In the soil used in this study, 9 of every 10 mm h⁻¹ of i_{sr-dr} at the soil surface represented lateral flow.

Consequently, in layered soil profiles in which the less permeable layer is located below the surface layer, i_{sr-dr} contains a significant amount of lateral flow and overestimates the effective saturated hydraulic conductivity of the soil profile. Hence, the use of this K_s would imply in inaccurate drainage, irrigation, and soil conservation designs.

Further studies comparing infiltration rate measurements from any technique with the saturated steady vertical flow rate estimated using the Richards equation would be useful to understand to what extent the measurements of infiltration are biased by natural and anthropic profile layering factors.

ACKNOWLEDGEMENT

This study was funded by the Coordenação de Aperfeiçoamento de Pessoal de Nível Superior (Capes) – Finance code 001.

AUTHOR CONTRIBUTIONS

Conceptualization:  Daniel Boeno (equal),  Paulo Ivonir Gubiani (equal), and  Quirijn de Jong Van Lier (equal).

Investigation:  Daniel Boeno (equal) and  Paulo Ivonir Gubiani (equal).

Methodology:  Daniel Boeno (equal).

Supervision:  Paulo Ivonir Gubiani (lead).

Writing - original draft:  Daniel Boeno (equal).

Writing - review & editing:  Paulo Ivonir Gubiani (equal),  Quirijn de Jong Van Lier (equal), and  Rodrigo Pivoto Mulazzani (equal).

REFERENCES

- Aboukarima AM, Al-Sulaiman MA, Marazky MSAE. Effect of sodium adsorption ratio and electric conductivity of the applied water on infiltration in a sandy-loam soil. *Water SA*. 2018;44:105-10. <https://doi.org/10.4314/wsa.v44i1.12>
- Ahuja LR, El-Swaify SA, Rahman A. Measuring hydrologic properties of soil with a double-ring infiltrometer and multiple-depth tensiometers. *Soil Sci Soc Am J*. 1976;40:494-9. <https://doi.org/10.2136/sssaj1976.03615995004000040016x>
- Alhameid A, Singh J, Sekaran U, Ozlu E, Kumar S, Singh S. Crop rotational diversity impacts soil physical and hydrological properties under long-term no- and conventional-till soils. *Soil Res*. 2020;58:84-94. <https://doi.org/10.1071/SR18192>
- Arriaga FJ, Kornecki TS, Balkcom KS, Raper RL. A method for automating data collection from a double-ring infiltrometer under falling head conditions. *Soil Use Manage*. 2009;26:61-7. <https://doi.org/10.1111/j.1475-2743.2009.00249.x>
- ASTM D3385-09. Standard test method for infiltration rate of soils in field using double-ring infiltrometer. West Conshohocken, PA: ASTM International; 2009. Available from: <https://www.astm.org/DATABASE.CART/HISTORICAL/D3385-09.htm>.
- Azooz RH, Arshad MA. Soil infiltration and hydraulic conductivity under long-term no tillage and conventional tillage systems. *Can J Soil Sci*. 1996;76:143-52. <https://doi.org/10.4141/cjss96-021>
- Bodhinayake W, Si BC, Noborio K. Determination of hydraulic properties in sloping landscapes from tension and double-ring infiltrometers. *Vadose Zone J*. 2004;3:964-70. <https://doi.org/10.2136/vzj2004.0964>
- Bonetti JA, Anghinoni I, Gubiani PI, Cecagno D, Moraes MT. Impact of a long-term crop-livestock system on the physical and hydraulic properties of an Oxisol. *Soil Till Res*. 2019;186:280-91. <https://doi.org/10.1016/j.still.2018.11.003>
- Bonini AK, Secco D, Santos RF, Reinert DJ, Reichert JM. Physical-hydraulic attributes and wheat yield in an Oxisol under compaction states. *Cienc Rural*. 2011;41:1543-8. <https://doi.org/10.1590/S0103-84782011005000122>
- Bouwer H. Intake Rate: Cylinder Infiltrometer. In: Kluter A, editor. *Methods of soil analysis: Part 1 - Physical and mineralogical methods*. 2nd ed. Madison: Soil Science Society of America; 1986. p. 825-44.
- Camara RK, Klein VA. Chiseling in no-tillage system as soil and water conservation practice. *Rev Bras Cienc Solo*. 2005;29:789-96. <https://doi.org/10.1590/S0100-06832005000500014>
- Cessa RMA, Souza MF, Brachtvogel EL, Souza FR, Panachuki E, Varão JH, Costa JS, Araújo ML, Caçol PSK. Velocidade de infiltração básica de água como indicador da qualidade porosa do solo. *Revista Agrogeoambiental*. 2014;6:83-92. <https://doi.org/10.18406/2316-1817v6n22014627>
- Chowdary VM, Rao MD, Jaiswal CS. Study of infiltration process under different experimental conditions. *Agr Water Manage*. 2006;83:69-78. <https://doi.org/10.1016/j.agwat.2005.09.001>
- Cunha JL, Coelho ME, Albuquerque AWD, Silva CA, Silva Júnior ABD, Carvalho ID. Water infiltration rate in Yellow Latosol under different soil management systems. *Rev Bras Eng Agr Amb*. 2015;19:1021-7. <https://doi.org/10.1590/1807-1929/agriambi.v19n11p1021-1027>
- Drescher MS, Eltz FLF, Denardin JE, Faganello A. Persistence of mechanical interventions effect for soil decompaction in no-tillage systems. *Rev Bras Cienc Solo*. 2011;35:1713-22. <https://doi.org/10.1590/S0100-06832011000500026>
- Drescher MS, Reinert DJ, Denardin JE, Gubiani PI, Faganello A, Drescher GL. Duration of changes in physical and hydraulic properties of a clayey Oxisol by mechanical chiseling. *Pesq Agropec Bras*. 2016;51:159-68. <https://doi.org/10.1590/S0100-204X2016000200008>
- Fatehnia M, Paran S, Kish S, Tawfiq K. Automating double ring infiltrometer with an Arduino microcontroller. *Geoderma*. 2016;262:133-9. <https://doi.org/10.1016/j.geoderma.2015.08.022>
- Fernández R, Frasier I, Quiroga A, Noellemeyer E. Pore morphology reveals interaction of biological and physical processes for structure formation in soils of the semiarid Argentinean Pampa. *Soil Till Res*. 2019;191:256-65. <https://doi.org/10.1016/j.still.2019.04.011>

- Franco GB. Environmental fragility and water quality of the Almada River Watershed - Bahia [thesis]. Viçosa, MG: Universidade Federal de Viçosa; 2010.
- Håkansson I. A method for characterizing the state of compactness of the plough layer. *Soil Till Res.* 1990;16:105-20. [https://doi.org/10.1016/0167-1987\(90\)90024-8](https://doi.org/10.1016/0167-1987(90)90024-8)
- Hillel D. Introduction to environmental soil physics. San Diego: Academic Press; 2004.
- Kovář P, Bačínová H, Loula J, Fedorova D. Use of terraces to mitigate the impacts of overland flow and erosion on a catchment. *Plant Soil Environ.* 2016;62:171-7. <https://doi.org/10.17221/786/2015-pse>
- Liu Y, Cui Z, Huang Z, López-Vicente M, Wu GL. Influence of soil moisture and plant roots on the soil infiltration capacity at different stages in arid grasslands of China. *Catena.* 2019;182:104147. <https://doi.org/10.1016/j.catena.2019.104147>
- Mbagwu JSC. Quasi-steady infiltration rates of highly permeable tropical moist savannah soils in relation to landuse and pore size distribution. *Soil Technol.* 1997;11:185-95. [https://doi.org/10.1016/s0933-3630\(96\)00138-9](https://doi.org/10.1016/s0933-3630(96)00138-9)
- Minosso J, Antoneli V, Freitas AR. Seasonal variability of water infiltration in soil in different types of use in the southeast region of Paraná. *Geografia Meridionalis.* 2017;03:86-103. <https://doi.org/10.15210/gm.v3i1.11041>
- Miyata S, Gomi T, Sidle RC, Hiraoka M, Onda Y, Yamamoto K, Nonoda T. Assessing spatially distributed infiltration capacity to evaluate storm runoff in forested catchments: Implications for hydrological connectivity. *Sci Total Environ.* 2019;669:148-59. <https://doi.org/10.1016/j.scitotenv.2019.02.453>
- Owuor SO, Butterbach-Bahl K, Guzha AC, Jacob S, Merbold L, Rufino MC, Pelster DE, Díaz-Pinés E, Breuer L. Conversion of natural forest results in a significant degradation of soil hydraulic properties in the highlands of Kenya. *Soil Till Res.* 2018;176:36-44. <https://doi.org/10.1016/j.still.2017.10.003>
- Pagliai M. Micromorphology and soils management. *Dev Soil Sci.* 1993;623-40. [https://doi.org/10.1016/s0166-2481\(08\)70449-5](https://doi.org/10.1016/s0166-2481(08)70449-5)
- Pott CA, De Maria IC. Comparison with field methods for assessing infiltration rates. *Rev Bras Cienc Solo.* 2003;27:19-27. <https://doi.org/10.1590/S0100-06832003000100003>
- Prando MB, Olibone D, Olibone APE, Rosolem CA. Water infiltration in soil as influenced by chiseling and crop rotations. *Rev Bras Cienc Solo.* 2010;34:693-700. <https://doi.org/10.1590/S0100-06832010000300010>
- Reynolds WD, Elrick DE, Youngs EG. Single-ring and double-or concentring-ring infiltrometers. In: Dane JH, Topp GC, editors. *Methods of soil analysis: Part 4 - Physical methods.* Madison: Soil Science Society of America; 2002. p. 821-6.
- Sales LEO, Ferreira MM, Oliveira MS, Curi N. Estimation of the soil basic infiltration velocity. *Pesq Agropec Bras.* 1999;34:2091- 5. <https://doi.org/10.1590/S0100-204X1999001100016>
- Santos HG, Jacomine PKT, Anjos LHC, Oliveira VA, Oliveira JB, Coelho MR, Lumberras JF, Cunha TJF. *Sistema brasileiro de classificação de solos.* 3. ed. rev. ampl. Rio de Janeiro: Embrapa Solos; 2013.
- Santos ILN, Filho RRG, Carvalho CM, Santos KV, Oliveira DTB, Souza LG. Water infiltration rate in soil grown in sweet corn with crotalaria coverage. *Rev Bras Agric Irrig.* 2016;10:925-34. <https://doi.org/10.7127/rbai.V10N500469>
- Schaap MG, Leij FJ, van Genuchten MT. Rosetta: A computer program for estimating soil hydraulic parameters with hierarchical pedotransfer functions. *J Hydrol.* 2001;251:163-76. [https://doi.org/10.1016/S0022-1694\(01\)00466-8](https://doi.org/10.1016/S0022-1694(01)00466-8)
- Schwartz RC, Schlegel AJ, Bell JM, Baumhardt RL, Evett SR. Contrasting tillage effects on stored soil water, infiltration and evapotranspiration fluxes in a dryland rotation at two locations. *Soil Till Res.* 2019;190:157-74. <https://doi.org/10.1016/j.still.2019.02.013>
- Sidiras N, Roth CH. Infiltration rate, measured with double-ring infiltrometers and a rainfall simulator, as affected by the amount of mulch and the tillage system. *Soil Till Res.* 1986;8:363. [https://doi.org/10.1016/0167-1987\(86\)90423-x](https://doi.org/10.1016/0167-1987(86)90423-x)

- Silva NF, Cunha FN, Filho FRC, Morais WA, Cunha ES, Roque RC, Alves DKM, Teixeira MB. Métodos para estimativa da infiltração de água em um Latossolo sob plantio direto e convencional. *GI Sci Technol*. 2017;10:169-76.
- Šimůnek J, van Genuchten MTh, Šejna M. The HYDRUS software package for simulating the two-and three-dimensional movement of water, heat, and multiple solutes in variably-saturated porous media. Riverside: Hydrus Technical Manual; 2012.
- Šimůnek J, van Genuchten MTh, Sejna M. The HYDRUS-1d software pack-age for simulating the one-dimensional movement of water, heat and multiple solutes in variably-saturated media. Version 3.0. Riverside: University of California Riverside; 2005.
- Šimůnek J, Šejna M, Saito H, Sakai M, van Genuchten MTh. The HYDRUS-1D software package for simulating the movement of water, heat, and multiple solutes in variably saturated media. Version 4.17. Riverside: University of California Riverside; 2013. (HYDRUS Software Series 3).
- Sithole NJ, Magwaza LS, Thibaud GR. Long-term impact of no-till conservation agriculture and N-fertilizer on soil aggregate stability, infiltration and distribution of C in different size fractions. *Soil Till Res*. 2019;190:147-56. <https://doi.org/10.1016/j.still.2019.03.004>
- Soil Survey Staff. Keys to soil taxonomy. 12th ed. Washington, DC: United States Department of Agriculture, Natural Resources Conservation Service; 2014.
- Stovin V, Poë S, De-Ville S, Berretta C. The influence of substrate and vegetation configuration on green roof hydrological performance. *Ecol Eng*. 2015;85:159-72. <https://doi.org/10.1016/j.ecoleng.2015.09.076>
- Suzuki LEAS, Reichert JM, Albuquerque JA, Reinert DJ, Kaiser DR. Dispersion and flocculation of Vertisols, Alfisols and Oxisols in Southern Brazil. *Geoderma Reg*. 2015;5:64-70. <https://doi.org/10.1016/j.geodrs.2015.03.005>
- Twarakavi NKC, Sakai M, Šimůnek J. An objective analysis of the dynamic nature of field capacity. *Water Resour Res*. 2009;45:W10410. <https://doi.org/10.1029/2009WR007944>
- Uloma AR, Samuel AC, Kingsley IK. Estimation of Kostiaikov's infiltration model parameters of some sandy loam soils of Ikwuano - Umuahia, Nigeria. *Open Trans Geosci*. 2014;1:34-8. <https://doi.org/10.15764/GEOS.2014.01005>
- Vilarinho MKC, Koetz M, Schlichting AF, Silva MC, Bonfim-Silva EM. Determination of water steady infiltration rate in native soil from Cerrado. *Rev Bras Agric Irrig*. 2013;7:17-26. <https://doi.org/10.7127/rbai.v7n100097>
- Wu L, Pan L, Roberson MJ, Shouse PJ. Numerical evaluation of ring-infiltrimeter under various soil conditions. *Soil Sci*. 1997;162:771-7. <https://doi.org/10.1097/00010694-199711000-00001>
- Youngs EG. Infiltration measurements - a review. *Hydrol Process*. 1991;5:309-19. <https://doi.org/10.1002/hyp.3360050311>
- Zhang J, Lei T, Chen T. Impact of preferential and lateral flows of water on single-ring measured infiltration process and its analysis. *Soil Sci Soc Am J*. 2016;80:859-69. <https://doi.org/10.2136/sssaj2015.12.0445>.
- Zhang J, Lei T, Qu L, Zhang M, Chen P, Gao X, Chen C, Yuan L. Method to quantitatively partition the temporal preferential flow and matrix infiltration in forest soil. *Geoderma*. 2019;347:150-9. <https://doi.org/10.1016/j.geoderma.2019.03.026>